NASA/TM—2014-216631

A Mathematical Model of Oxygen Transport in Skeletal Muscle During Hindlimb Unloading

Laura Causey
The City College of New York, New York, New York

Beth E. Lewandowski
Glenn Research Center, Cleveland, Ohio

Sheldon Weinbaum
The City College of New York, New York, New York

March 2014

NASA STI Program . . . in Profile

Since its founding, NASA has been dedicated to the advancement of aeronautics and space science. The NASA Scientific and Technical Information (STI) program plays a key part in helping NASA maintain this important role.

The NASA STI Program operates under the auspices of the Agency Chief Information Officer. It collects, organizes, provides for archiving, and disseminates NASA's STI. The NASA STI program provides access to the NASA Aeronautics and Space Database and its public interface, the NASA Technical Reports Server, thus providing one of the largest collections of aeronautical and space science STI in the world. Results are published in both non-NASA channels and by NASA in the NASA STI Report Series, which includes the following report types:

- TECHNICAL PUBLICATION. Reports of completed research or a major significant phase of research that present the results of NASA programs and include extensive data or theoretical analysis. Includes compilations of significant scientific and technical data and information deemed to be of continuing reference value. NASA counterpart of peer-reviewed formal professional papers but has less stringent limitations on manuscript length and extent of graphic presentations.

- TECHNICAL MEMORANDUM. Scientific and technical findings that are preliminary or of specialized interest, e.g., quick release reports, working papers, and bibliographies that contain minimal annotation. Does not contain extensive analysis.

- CONTRACTOR REPORT. Scientific and technical findings by NASA-sponsored contractors and grantees.

- CONFERENCE PUBLICATION. Collected papers from scientific and technical conferences, symposia, seminars, or other meetings sponsored or cosponsored by NASA.

- SPECIAL PUBLICATION. Scientific, technical, or historical information from NASA programs, projects, and missions, often concerned with subjects having substantial public interest.

- TECHNICAL TRANSLATION. English-language translations of foreign scientific and technical material pertinent to NASA's mission.

Specialized services also include creating custom thesauri, building customized databases, organizing and publishing research results.

For more information about the NASA STI program, see the following:

- Access the NASA STI program home page at *http://www.sti.nasa.gov*

- E-mail your question to *help@sti.nasa.gov*

- Fax your question to the NASA STI Information Desk at 443–757–5803

- Phone the NASA STI Information Desk at 443–757–5802

- Write to:
  STI Information Desk
  NASA Center for AeroSpace Information
  7115 Standard Drive
  Hanover, MD 21076–1320

NASA/TM—2014-216631

A Mathematical Model of Oxygen Transport in Skeletal Muscle During Hindlimb Unloading

Laura Causey
The City College of New York, New York, New York

Beth E. Lewandowski
Glenn Research Center, Cleveland, Ohio

Sheldon Weinbaum
The City College of New York, New York, New York

National Aeronautics and
Space Administration

Glenn Research Center
Cleveland, Ohio 44135

March 2014

Level of Review: This material has been technically reviewed by technical management.

Available from

NASA Center for Aerospace Information
7115 Standard Drive
Hanover, MD 21076–1320

National Technical Information Service
5301 Shawnee Road
Alexandria, VA 22312

Available electronically at http://www.sti.nasa.gov

A Mathematical Model of Oxygen Transport in Skeletal Muscle During Hindlimb Unloading

Laura Causey
The City College of New York
New York, New York 10031

Beth E. Lewandowski
National Aeronautics and Space Administration
Glenn Research Center
Cleveland, Ohio 44135

Sheldon Weinbaum
The City College of New York
New York, New York 10031

Abstract

During hindlimb unloading (HU) dramatic fluid shifts occur within minutes of the suspension, leading to a less precise matching of blood flow to O_2 demands of skeletal muscle. Vascular resistance directs blood away from certain muscles, such as the soleus (SOL). The muscle volume gradually reduces in these muscles so that eventually the relative blood flow returns to normal. It is generally believed that muscle volume change is not due to O_2 depletion, but a consequence of disuse. However, the volume of the unloaded rat muscle declines over the course of weeks, whereas the redistribution of blood flow occurs immediately. Using a Krogh Cylinder Model, the distribution of O_2 was predicted in two skeletal muscles: SOL and gastrocnemius (GAS). Effects of the muscle blood flow, volume, capillary density, and O_2 uptake, are included to calculate the pO_2 at rest and after 10 min and 15 days of unloading. The model predicts that 32 percent of the SOL muscle tissue has a $pO_2 < 1.25$ mmHg within 10 min, whereas the GAS maintains normal O_2 levels, and that equilibrium is reached only as the SOL muscle cells degenerate. The results provide evidence that there is an inadequate O_2 supply to the mitochondria in the SOL muscle after 10 min HU.

Introduction

In 1992 McDonald et al. wrote two papers describing how blood flow is redirected upon 15 days of hindlimb unloading (HU) in the rat (Refs. 1 and 2). Hindlimb unloading is of interest since it mimics aspects of microgravity by removing weightbearing loads from the hindlimbs and produces a cephalic fluid shift, similar to that which occurs in astronauts in a microgravity environment (Refs. 3 and 4). Both papers evaluated the possibility that the changes in perfusion to the soleus (SOL) and gastrocnemius (GAS) muscle during HU contributed to their degeneration. Hindlimb unloading reduces the release of vasodilatory metabolites, such as nitric oxide, and decreases the responsiveness of the sympathetic nervous system. These actions change the blood flow path (Refs. 1 and 2). The first study compared the blood flow and perfusion rate (blood flow relative to the muscle weight) to the SOL in standing, 10 min HU (the control group), and 15 day HU rats (Ref. 2). The group found that the relative blood flow to the SOL in the 15 day HU rats was higher than what was considered to be the control group (10 vs. 8 mL × (min × 100 g)$^{-1}$, respectively). The second study examined these parameters in 15 day HU and cage-controlled rats and concluded that the relative flow to the 15 day HU rats was about the same as the control (12 vs. 20 × (min × 100 g^{-1}, respectively)) (Ref. 1) even though the relative flow was reduced by

40 percent. The studies mutually concluded that the fatigability of the SOL was not a result of reduced muscle blood flow.

Upon a closer look, this deduction is problematic. The studies neglected to compare the O_2 uptake of the SOL to the O_2 delivery to determine if the muscle was adequately oxygenated. Furthermore, one study assumed that the rats that underwent 10 min of HU would be adequate controls and that in these animals the SOL was sufficiently perfused and oxygenated (Ref. 2). An analysis by Bloomfield et al., 2006 based on data collected by Colleran et al., 2000 reviewed how the perfusion rate to the SOL changes after 10 min, 7 days, and 28 days HU in a rat (Refs. 5 and 6). The study found that the vast majority (>80 percent) of the perfusion rate changes when moving from a standing to a HU position within the first 10 min.

In this analysis, the data predominately from the aforementioned studies was reexamined to consider the possibility that hypoxia in the SOL may cause adverse effects, such as degeneration. Due to limited information regarding how the O_2 uptake in the rat SOL changes upon HU and exercise, the scope was narrowed to predict only the percentage of the SOL that becomes hypoxic if this muscle maintains normal resting metabolism as it would on earth. This is contrary to that which actually occurs during spaceflight since slow twitch SOL muscles transition to fast-twitch muscles. For example, after 5 weeks of hindlimb suspension, the maximum rate of O_2 uptake is decreased by 19 percent in the SOL muscle (Ref. 7). Further, there is evidence in the SOL of a cat that suggests that as muscle perfusion is diminished there is a downregulation in O_2 uptake (Ref. 8). Despite this, the model provides evidence that within the first week of HU the SOL cannot maintain a normal resting metabolism without facing the consequences of partial tissue hypoxia. It therefore seems plausible that an O_2 deficit may have adverse results on this muscle during HU.

Methods

The extent of hypoxia was first estimated by treating the tissue and blood as well-mixed regions. Table 1 lists the flowrate, Q, perfusion rate, Q/M_T, and volume, V_T, of the SOL and GAS at rest and after 10 min and 15 days of HU, as recorded by the two studies by McDonald, et al., 1992 (Refs. 1 and 2). The volume was determined by dividing Q into Q/M_T and assuming that the density of muscle is 1.056 g × cm^{-3}.

Arterial blood is normally saturated with O_2 so that the concentration of O_2 is $C_aO_2 = 0.2\ mL_{O2/}mL_{blood}$. To estimate the O_2 supply to each muscle Q/M_T data from the two McDonald, et al., 1992 studies were multiplied by this value, so that O_2 Supply = $0.2\ mL_{O2}/mL_{blood} \times Q/M_T$. The O_2 uptake of SOL and GAS are 2.2 mL_{O2}/(100 g × min) and 0.8 mL_{O2}/(100 g × min), respectively (Refs. 9 and 10). The O_2 supply for each muscle was plotted at rest and after 10 min and 15 days of HU and compared with the O_2 uptake of the respective muscles. The results of this calculation are plotted in Figure 2.

The calculations using a spatially lumped region depend on the fact that the radial gradient of pO_2 is quite small, which was checked using the Krogh model in which the tissue surrounding each capillary is treated as a cylinder. The validity of the assumptions made for this spatially lumped region model are analyzed in the discussion.

TABLE 1.—FLOW AND TISSUE VOLUME FROM MCDONALD, ET AL., 1992 STUDIES

	Resting			10 min HU			15 days HU			Ref.
	Q[a]	Q/M_T[b]	V_T cm^3	Q[a]	Q/M_T[b]	V_T cm^3	Q[a]	Q/M_T[b]	V_T cm^3	
SOL	----	----	----	1.6	8.0	0.19	0.8	10.0	0.08	(Ref. 2)
	3.7	20.0	0.18	----	---	----	1.3	12.0	0.10	(Ref. 1)
GAS	----	----	----	13.3	7.1	1.79	13.6	9.2	1.40	(Ref. 2)
	26.1	12.4	1.99	----	---	----	23.6	14.9	1.50	(Ref. 1)

[a] Q is in units of mL × (100 × min)$^{-1}$

[b] Q/M_T is in units of mL × (100 g × min)$^{-1}$

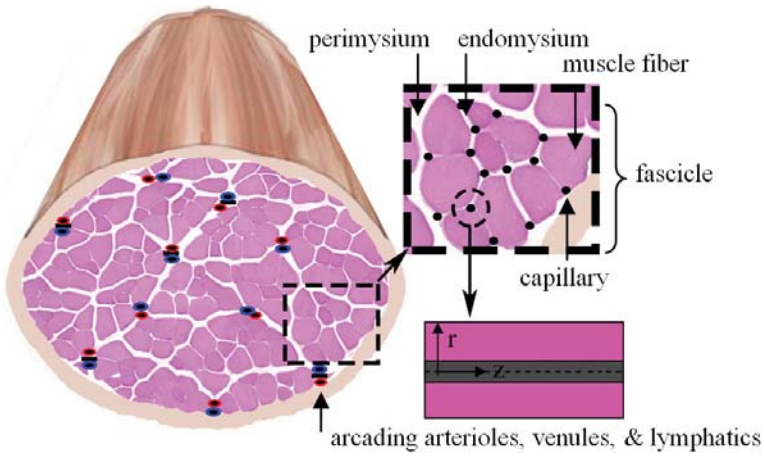

Figure 1.—Krogh cylinder cross-section with dimensions labeled.

The cross section parallel to the axial direction of a Krogh cylinder is shown in Figure 1, with dimensions labeled. To find the amount of oxygen in a given physical system a mass balance was performed. In Equation (1) the change in oxygen concentration with respect to time is equal to the gradient of the mass flux of the oxygen minus the rate of oxygen uptake by the muscle fibers, written as,

$$\partial C / \partial t = -\nabla \cdot n - R . \tag{1}$$

The mass flux of the system is a sum of the diffusive flux, according to Fick's Law of Diffusion, and the convective flux where D is the diffusivity and v_0 is the volume average velocity, given by,

$$n = -D\nabla C + Cv_0 . \tag{2}$$

Using Equations (1) and (2) the change in oxygen concentration per unit time is

$$\partial C / \partial t = -\nabla \cdot \left(-D\nabla C + Cv_0\right) - R . \tag{3}$$

Equation (3) was used to determine the mass balance of oxygen in the capillaries and tissue. A detailed description of the Krogh cylinder calculations can be found in Reference 41. Calculations are briefly described for this Krogh Cylinder problem.

Tissue

In the tissue a number of assumptions were made to simplify the problem: (1) steady state system, (2) negligible convection effects, and (3) diffusion in the axial direction is neglected. Henry's Law was used to express the concentration of oxygen in terms of partial pressure ($pO_2 = C \times H$). The boundary conditions were set for this equation. At the interface between the capillary and tissue ($r = r_c$) the partial pressure of oxygen is the same ($pO_2 = pO_2^T$) and the oxygen flux is continuous ($D \times \partial pO_2/\partial r = D^T$ x $\partial pO_2^T/\partial r$). At the Krogh tissue cylinder diameter ($r = r_T$) the flux is zero ($\partial pO_2^T/\partial r = 0$) since there is a plane of symmetry between cylinders. When the level of O_2 in the muscle tissue reaches a state in which $pO_2^T = 0$ it will not continue to uptake O_2 since there is no O_2 to be taken and it is impossible to have a negative oxygen distribution. To account for this, r_T (z) was replaced with r_a (z) (the radius at which tissue becomes anoxic) in cases in which the tissue became anoxic at a given radius along the length of the tissue cylinder. After applying the aforementioned assumptions and boundary conditions Equation (3) becomes

$$pO_2^T(r,z) = pO_2(z) - RH^T / 4D^T \left[r_c^2 - r^2 - 2r_T(z)^2 \ln(r / r_c) \right] , \quad (4)$$

for $r_C < r < r_T$,where $pO_2(z)$ is the partial pressure of oxygen in the capillary, H is Henry's Constant, and T denotes the properties of the tissue.

Capillary

Equation (3) was used to solve for the concentration of oxygen in the blood by assuming: (1) steady state, (2) no convection in the radial direction, and (3) axial diffusion is negligible when compared with axial convection. The mass balance for concentration of hemoglobin was found using Equation (3) as well, replacing C with C', with the apostrophe denoting that it is the concentration of hemoglobin. Some key assumptions were made: (1) steady state, (2) no diffusive transport of hemoglobin, and (3) negligible change in the concentration of hemoglobin in the radial direction. It was assumed that there was adequate conductive mixing of O_2 in the plasma. The mass balance of the oxygen was combined with that of the hemoglobin by recognizing that the rate of disappearance of oxygenated hemoglobin must equal the rate of appearance of dissolved oxygen. Henry's Law was used to represent the equation in terms of the partial pressure of oxygen. Equation (5) is the result where m is the change in hemoglobin concentration with respect to the oxygen concentration, as given by,

$$\partial pO_2 / \partial z = D / (v_0(1+m)) \left[1 / r \times \partial / \partial r \left(r \times \partial pO_2 / \partial r \right) \right] . \quad (5)$$

The boundary condition was applied which states that at the capillary radius the flux of the oxygen is continuous and the radial average of the oxygen within the capillary was taken since the bulk of the mass transfer resistance is in the tissue and not the capillary (Ref. 11), leading to

$$d\left\langle pO_2 \right\rangle / dz = 2D^T / (v_0(1+m) r_c) dpO_2^T / dr \,|_{r_c} . \quad (6)$$

The term dpO_2^T/dr was found by taking the derivative of Equation (4) with respect to r and evaluating it at r_c. An additional boundary condition was applied since at the capillary entrance ($z = 0$) $\langle pO_2 \rangle_{in}$ is known. Using these methods, the partial pressure of oxygen within the capillary for $0 < z < L$ is

$$\left\langle pO_2(z) \right\rangle = \left\langle pO_2 \right\rangle_{in} - RH^T / (v_0(1+m)) \left[r_T(z)^2 / r_c^2 - 1 \right] z \quad . \quad (7)$$

Oxygen-Hemoglobin Dissociation Curve and Myoglobin Effects

The effects of the O_2 carrying proteins, hemoglobin and myoglobin, were considered. Oxygen dissociates from hemoglobin as O_2 is lowered, enhancing its availability. The Hill Equation (Equation (B7) in the Appendix) was used to calculate the dependence of the slope of the O_2-hemoglobin dissociation curve (m) on the pO_2 along the length of the capillary. We used the average m value for the range of pO_2 considered (0 to 71 mmHg normally and 0 to 64 mmHg in environmental hypoxic conditions, as will be discussed shortly) along the length of the capillary. Myoglobin enhances O_2 transport at low O_2 concentrations. At critical O_2 concentration myoglobin-assisted transport is greatest at which point the diffusivity is enhanced by a factor of 1.06 in skeletal muscle (Ref. 12). If any portion of the SOL or GAS reached levels <1.25 mmHg the diffusion coefficient was multiplied by this factor to account for the modest myoglobin effect.

Parameters

The perfusion rate equals the flowrate of blood per unit volume of the total muscle, Q/V_T. Therefore, the velocity of the blood flowing through each capillary, v_0, is

$$v_0 = Q \times r_T^2 \times L / \left(V_T \times r_C^2 \right) . \tag{8}$$

The Q, V_T, and r_T were variable, whereas other parameters in this equation remained constant.

The tissue cylinder radius, r_T, was calculated by assuming that the capillaries within the skeletal muscle are evenly spaced. The calculation for r_T is

$$\pi r_T^2 = 1/nc , \tag{9}$$

where nc is capillary density. The capillary density in the SOL and GAS muscles of the rat is 836 and 628 capillaries/mm^2, respectively (Refs. 13 and 14). The results of this calculation are listed in Table 2.

Literature values for the capillary density of rats under HU conditions were used for both muscles to estimate the tissue cylinder radius after 15 days HU. The capillary density in the SOL muscles of the rat after HU for 9 days is 994 capillaries/mm^2 (Ref. 13). It was assumed that this value would not change significantly after 6 more days. We inserted this value into Equation (9). After 10 days of HU in the GAS of a mouse the capillary to fiber ratio decreases by 19.5 percent (Ref. 21). However, after 15 days the volume of the GAS muscle changes from 1.99 to 1.50 cm^3. Equation (10) was used to estimate the r_T in the GAS muscle of the hindlimb unloaded rat after 15 days and is given by

$$\pi r_T^2 = \left(1.50/1.99\right) / \left(628/\text{mm}^2 \times \left(1 - 0.195\right) \right) . \tag{10}$$

The values for the muscle tissue cylinder radii are listed in Table 2.

TABLE 2.—MODEL PARAMETERS

Parameter	Value	Source
D^T	1.65 to 3.04×10^{-5} cm^2/s	(Refs. 15 and 16)
N	2.64	(Ref. 17)
pO_{50}	26.2	(Ref. 17)
C_{sat}	8800 μM	(Ref. 18)
H, H^T[b]	0.74 mmHg/μM	(Ref. 18)
$pO_{2,in}$ (normal)	71.4 mmHg	(Ref. 19)
$pO_{2,in}$ (HYP)	64.4 mmHg	a
L	500 μm	(Ref. 20)
r_c	2.5 μm	(Ref. 20)
R_{sol}	17.04 μM/s	a
R_{gas}	6.20 μM/s	a
$r_{T,sol}$ (normal)	20 μm	a
$r_{T,gas}$ (normal)	23 μm	a
$r_{T,sol}$ (15 days HU)	18 μm	a
$r_{T,gas}$ (15 days HU)	22 μm	a

[a]Calculated

[b]Assumed that $H = H^T$

Groebe and Thews (1990) suggested that extracellular and intracellular pO_2 diffusivities are different. They referred to the space containing plasma, capillary endothelium, and interstitial space as the "perierythrotic regions" and claimed that the diffusivity of this region, 1.65×10^{-5} cm^2/s (Ref. 15), has higher diffusion properties than that within the myocyte, which was assumed to be comparable to water (3.04×10^{-5} cm^2/s) (Ref. 16). The Krogh Cylinder Model was used to compare the percent volume of the tissue that becomes hypoxic using these two diffusion coefficients.

The amount of O_2 extracted from the blood in resting SOL and GAS muscles is 2.2/20.0 mL_{O2}/mL_{bl} (equivalent to 4840 μM) and 0.8/12.4 mL_{O2}/mL_{blood} (equivalent to 2839 μM), respectively. The rate of O_2 uptake of the resting SOL muscle tissue may be estimated as

$$R_{sol} = \frac{20\,\mathrm{mL_{bl}}}{100\,\mathrm{g}\times 60s}\times 4840\,\mu\mathrm{M}\times\frac{1.056\,\mathrm{g}}{\mathrm{cm}^3}\times\frac{1000\,\mathrm{cm}^3}{L_{\mathrm{tiss}}}\times\frac{\mu\mathrm{mol}}{\mathrm{L_{bl}}\mu\mathrm{M}}\times\frac{1\,\mathrm{L_{bl}}}{1000\,\mathrm{mL_{bl}}} = 17.04\frac{\mu\mathrm{M}}{s}. \qquad (11)$$

The rate of O_2 uptake of the GAS muscle tissue was similarly found to be 6.20 μM/s. The model parameters are listed in Table 2. The parameters pO_{50}, C_{sat}', and N were used to calculate the slope of the O_2-hemoglobin dissociation curve (m) in Equation (B7), as discussed in Appendix B.

Simulated Hypoxic Environmental Conditions

Astronauts perform a pre-breathe protocol to remove nitrogen from the body before a spacewalk. To minimize the pre-breathe time crewmembers may live in an atmosphere that has a low partial pressure of nitrogen, which can be achieved at lower ambient pressures. To analyze this effect in our model, we considered a case in which the atmospheric pressure is lowered from 14.7 to 8 psi and the O_2 concentration is raised from 21 to 32 percent, causing the cabin partial pressure of O_2 to be reduced.

The normal partial pressure of O_2 in air is: 760 mmHg × 0.21 = 159 mmHg. Under these normal conditions, the partial pressure of O_2 that enters the capillary bed of the muscle is ~71.4 mmHg (Ref. 19) since there is a longitudinal gradient of pO_2 in precapillary microvessels (Ref. 22). If we lower the cabin pressure to 414 mmHg and increase the O_2 concentration to 32 percent, the partial pressure of O_2 is 132 mmHg. The arterial blood partial pressure of O_2 was measured by Fisher, et al., 1992 in a rat after it was exposed to various degrees of hypoxia. Data excerpts from the aforementioned study are listed in Table 3. To estimate the arterial pO_2 for an inspired partial pressure of O_2 of 132 mmHg (the equivalent of 17 percent O_2 at a cabin pressure of 760 mmHg) a curve was fitted to the data from Table 3. We found the arterial pO_2 to be approximately 64.4 mmHg. We used this value as an input for our model.

Mathematical Model

MATLAB (V. R2007b, MathWorks, Natick, MA) software was used to perform the calculations. The pO_2 at the capillary entrance was assigned and it was first assumed that there were no hypoxic areas. The pO_2 in the capillary and tissue was then calculated. If $pO_2^T < 0$ at any point along the capillary $r_T(z)$ was reduced to a value $r_a(z)$ at that location and the model was iterated once again.

TABLE 3.—ARTERIAL PO_2 AT DIFFERENT O_2 CONCENTRATIONS
(Data from Fisher, et al., 1992)

	10%	21%	30%
Arterial pO_2, mmHg	55.1	71.4	91.4

Results

The first analysis of data that we made treated the tissue and blood as well-mixed regions. In a resting state both the SOL and GAS O_2 supplies exceed the demand by 1.8 mL/(min × 100 g) and 1.7 mL/(min × 100 g), respectively, assuming that the radial gradient of pO_2^T is negligible. After 10 min of HU the flow in the SOL and GAS is reduced from 20.0 and 12.4 mL/(min × 100 g) to 8.0 and 7.1 mL/(min × 100 g) and the O_2 supply becomes 1.6 and 1.4 mL/(min × 100 g), respectively, as shown in Figure 2 (Refs. 1 and 2). In the case of the SOL this means that portions of the muscle may become hypoxic, assuming normal muscle metabolism is maintained, whereas the GAS is adequately perfused. After 15 days HU the SOL and GAS experience a 44 to 58 percent and 22 to 25 percent volume decrease. The O_2 deficit is ameliorated by the reduced muscle volume.

The distribution of O_2 within a cross-section of the Krogh tissue cylinder in the SOL and GAS muscles is represented by Figure 3. The arrow located at the bottom left-hand corner indicates the location at which the "simulated blood" enters the Krogh cylinder cross-section at $z = 0$. At this point normally $pO_{2,in} = 71.4$ mmHg. The space in which the blood is flowing is from $r = 0$ to 2.5 μm and $z = 0$ to 500 μm. The endomysial and perimysial tissue resides in the space from $r = 2.5$ μm to r_T. The partial pressure of O_2 was color coded to indicate the pO_2^T. The partial pressure of O_2 at which mitochondrial metabolism becomes inhibited in the muscle is ~1.25 mmHg (Ref. 23). The black region represents the portion of the tissue reduced below this level.

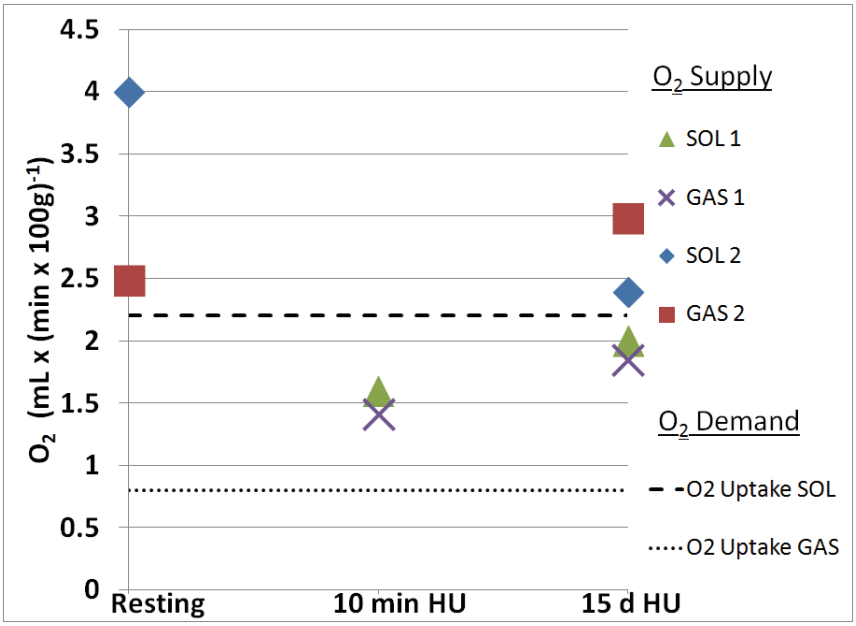

Figure 2.—Comparison of O_2 supply and demand. SOL 1, GAS 1 data from Reference 1; SOL 2, GAS 2 data from Reference 2. The O_2 demand in the SOL and GAS was experimentally determined by References 9 and 10.

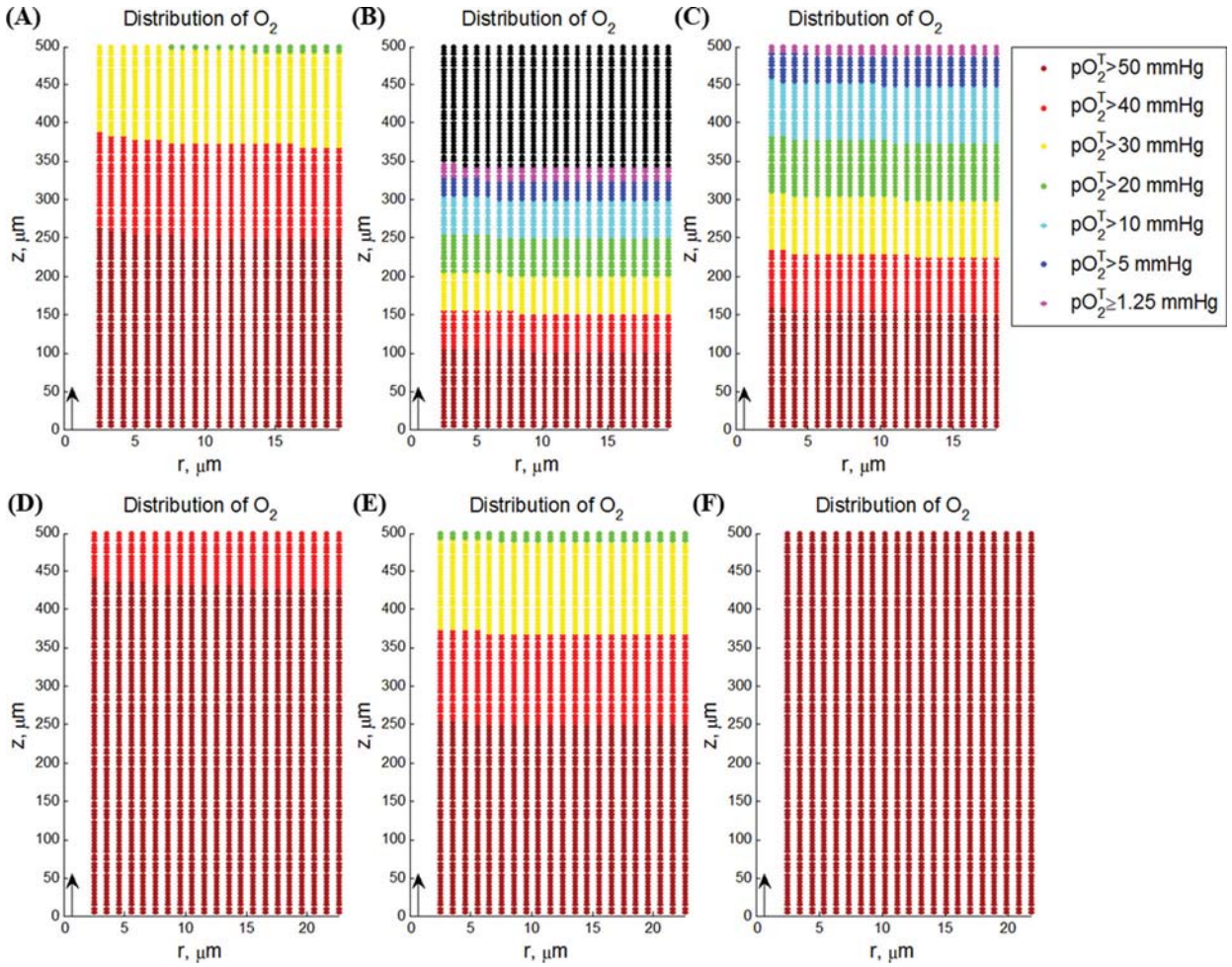

Figure 3.—Distribution of O_2 in the SOL (A to C) and GAS (D to F) muscles. The left-most plots (A and D) depict the resting tissue. The center plots (B and E) show the tissue after the blood flow is redistributed after 10 min HU. The right-most plots depict the tissue when the blood flow and volume of the muscle has been reduced after 15 days HU. The mean pO_2^T for each plot was (A) 50 mmHg, (B) 25 mmHg, (C) 37 mmHg, (D) 59 mmHg, (E) 50 mmHg, and (F) 61 mmHg. The percent volume of the tissue that is hypoxic in (B) is 32 percent. ($D^T = 3.04\times10^{-5}$ cm^2/s). Note that (C) and (F) were generated using data from Reference 1.

Normal Conditions

The model predicts that the average pO_2^T in the SOL and GAS muscles during normal conditions is 50 and 59 mmHg, respectively. Experimentally, the average SOL and GAS intramuscular pO_2^T is ~51 mmHg in the rat (Ref. 24) and ~48 mmHg in the canine (Ref. 25), respectively. We estimate that the pO_2^T in the SOL muscle ranges from 30 to 71 mmHg and the GAS muscle has a pO_2^T from 47 to 71 mmHg. During normal resting conditions the SOL muscle is perfused by blood over 1.5 times that of the amount of blood perfused to the GAS muscle per tissue weight (Ref. 1). The capillary density of the SOL and GAS muscles are nearly the same. Therefore, the reason the level of pO_2^T is less in SOL muscle as compared with the GAS is almost entirely attributed to the differences in O_2 consumption of the two muscles. To achieve our results, the value of tissue diffusivity, D^T, was first assumed to be that of water, 3.04×10^{-5} cm^2/s (Ref. 16). This is the best possible scenario since the D^T is equal to 1.65×10^{-5} cm^2/s at the wall of the capillary (Ref. 15). The influence of D^T on the O_2 distribution was further analyzed, as described shortly.

10 min—Most of the changes in blood flow that arise in the SOL and GAS muscles during HU occur within a timeframe of 10 min of weightlessness (Ref. 5). When the blood flow changes due to HU the O_2 distribution is reduced, as shown in Figure 3(B) and (E). The percent volume of the SOL in which pO_2^T <1.25 mmHg is 32 percent. Our model predicts that the average pO_2^T in the SOL and GAS muscles is 25 and 50 mmHg, respectively. The pO_2^T in the SOL muscle ranges from 0 to 71 mmHg and the GAS muscle has a pO_2^T from 29 to 71 mmHg; still within a normal range.

15 days—Within weeks of decreased blood flow, the muscle volume decreases in both muscles. Using our model, we found that the average pO_2^T in the SOL and GAS muscles when the blood flow and muscle volume were changed to the values provided by Reference 1 and the capillary density was changed to the HU values listed in Table 2 was 37 and 61 mmHg, respectively. The pO_2^T in the SOL and GAS muscles ranged from 3 to 71 and 51 to 71 mmHg, respectively.

Similarly, the mean pO_2^T predicted using values from Reference 2 was 31 mmHg for the SOL and 55 mmHg for the GAS. In the same study the pO_2^T in the SOL and GAS muscles ranged from 0 to 71 and 39 to 71 mmHg, respectively. Figure 3(C) and (F) demonstrate that the pO_2^T returns to higher oxygenation levels after the volume of the muscle is reduced as compared with Figure 3(B) and (E). According to Reference 1 this O_2 distribution is only achieved if the SOL and GAS experience a 44 and 25 vol% decrease, respectively.

Simulated Hypoxic Environmental Conditions

When the partial pressure of O_2 is decreased to 132 mmHg, the slightly hypoxic environment reduces the O_2 distribution so that the range of pO_2^T is 26 to 64 and 42 to 64 mmHg in the SOL and GAS, respectively.

10 min—The exposure to a hypoxic environment in addition to the changes in the distribution of blood flow causes further O_2 depletion in the tissue. In this scenario, the SOL and GAS muscle pO_2^T ranges from 0 to 64 and 26 to 64 mmHg, respectively. The average pO_2^T for the SOL and GAS after these changes is 22 and 45 mmHg, respectively.

15 days—In the same environment the O_2 distribution was predicted after the blood flow and volume were changed and the muscle reaches a state of equilibrium using the data from the two studies listed in Table 1. When the perfusion rate of Reference 1 was used in the model the pO_2^T in the SOL and GAS muscles ranged from 2 to 64 and 46 to 64 mmHg, respectively. The average pO_2^T in the SOL and GAS was predicted to be 33 and 55 mmHg, respectively. Using data from Reference 2, the pO_2^T in the SOL and GAS muscles ranged from 0 to 64 and 35 to 64 mmHg and the average pO_2^T was predicted to be 28 and 49 mmHg, respectively. Table 4 shows the estimated percentage of the tissue that has an O_2 deficit under these different circumstances for $D^T = 3.04\times10^{-5}$ cm^2/s.

TABLE 4.—PERCENTAGE OF HYPOXIC TISSUE IN DIFFERENT CONDITIONS IN THE SOL

	% Hypoxic tissue $D^T = 3.04\times10^{-5}$ cm^2/s	% Hypoxic tissue $D^T = 1.65\times10^{-5}$ cm^2/s
Resting[b]	0.0	0.0
Resting[b] HYP	0.0	0.0
10 min HU[a]	31.7	32.5
10 min HU[a] HYP	33.2	34.0
15 days[a]	14.6	15.4
15 days[a] HYP	15.8	16.7
15 days[b]	0.0	0.0
15 days[b] HYP	0.0	0.6

[a]Mcdonald, et al., 1992 (Ref. 2)
[b]Mcdonald, et al., 1992 (Ref. 1)

The Krogh Cylinder was evaluated for each circumstance in the SOL using two different diffusion coefficients. After 10 min HU in an ambient environment there was 31.7 and 32.5 percent hypoxic tissue when $D^T = 1.65\times10^{-5}$ and 3.04×10^{-5} cm^2/s, respectfully. This information suggests that the percentage of hypoxic tissue is mostly dependent on the tissue perfusion with the tissue diffusivity being a less important factor.

Discussion

In order for long duration human space exploration, such as from Earth to Mars, to become a reality, the impact of the missions on the health of the astronauts needs to be understood and mitigated. Since limited astronaut spaceflight data exists and is difficult to obtain, other ground-based methods have been established to simulate spaceflight conditions, such as HU.

The conventional belief is that during spaceflight muscle fibers atrophy and, due to a smaller fiber diameter, the distance between the O_2 in blood residing in the capillaries and the mitochondria decreases, improving O_2 transport (Ref. 26). However, the blood is redistributed within the first 10 min of HU (Ref. 5), while the capillary density and muscle volume changes are observed after at least one and two weeks have passed, respectively (Refs. 2 and 1). There are two reasons that the muscle decreases in volume: short-term redistribution of fluids in the interstitium and long-term muscle degeneration (Ref. 27). Dramatic fluid shifts occur within minutes of arriving in microgravity. During this time the hydrostatic pressure in the vascular system of the legs decreases and fluid from the interstitium is reabsorbed into the vascular system, as described by Starling's Principle (Ref. 5). However, this action accounts for only 4 percent of the total SOL muscle loss whereas the remaining 96 percent of the total muscle volume lost occurs due to the downregulation of protein synthesis or muscle atrophy, which is measured over the course of weeks in rats (Ref. 28). Therefore, the distance between the capillary and the muscle fiber does not decrease immediately. In the past the conclusion was made that since the volume of the muscle changes, the capillaries are able to fully oxygenate the adjacent muscle fibers since the distance between them is reduced (Ref. 26). However, as we show, the oxygen is depleted from the muscle after the blood flow is redistributed within the first 10 min. By analyzing the O_2 distribution using a mathematical model that simulates the fluid shift, the O_2 distribution was predicted at different timeframes. The results support the idea that the O_2 equilibrium is reached only as the muscle fibers degenerate.

The redistribution of blood flow in the SOL and GAS muscle upon HU is most likely acutely due to a reduced release of vasodilatory metabolites, such as nitric oxide (Ref. 2). The chronic decreased responsiveness of the sympathetic nervous system is responsible for the inadequate regulation of blood flow in the long-term (Refs. 1 and 2). In the rat, muscle composed primarily of fast-twitch fibers has the potential for greater control of vascular tone by the sympathetic nervous system than that composed of slow-twitch fibers. Thus, a reduction in sympathetic mediated vascular tone would be expected to increase blood flow to muscle composed of fast-twitch fibers (Ref. 2).

In skeletal muscle cells (also referred to as fibers), the mitochondria require O_2 to undergo mitochondrial oxidative phosphorylation, the main source of ATP for a muscle fiber. The partial pressure of O_2 at which mitochondrial metabolism becomes inhibited in skeletal muscle is ~1.25 mmHg (Ref. 23). When O_2 is limited ATP generation begins to diminish but the cellular demands remain constant, leading to an energy deficit. This can be temporarily ameliorated by anaerobic ATP production. Certain muscle types are more successful than others in this regard. Type I (slow-twitch) fibers have many mitochondria, a high concentration of myoglobin, and a low glycolytic capacity so that they principally respire aerobically. Type II (fast-twitch) fibers rely mostly on anaerobic respiration (Ref. 26). Type IIA fibers have a high glycolytic capacity and a moderate oxidative activity whereas type IIB have a high glycolytic capacity and a low oxidative capacity. The SOL muscle contains approximately 91 percent type I fibers and 9 percent type IIA fibers whereas the GAS consists of 18 percent type I fibers, 30 percent type IIA fibers and 52 percent type IIB fibers (Ref. 29). Therefore, the SOL is more dependent on O_2 than the GAS to generate ATP (Ref. 30). If ATP production does not meet the energetic demands the cell may survive

only if it is able to initiate mechanisms that preserve its ionic integrity. Since protein synthesis is a major ATP sink it is a target for downregulation (Ref. 31). In microgravity muscle degeneration can be attributed to protein loss primarily due to a decline in protein synthesis (Refs. 32 and 33).

The validity of using a Krogh cylinder to estimate O_2 transport in a muscle has been debated. Ellis et al., 1983 questioned the Krogh cylinder approach to O_2 diffusion given the substantial tortuosity and branching of the skeletal muscle capillary bed. A mathematical model for the transport of O_2 in a contracted muscle becomes complicated since the capillaries become tortuous as the muscle shortens (Ref. 34). This finding limits the mathematical model described herein so that it is only valid for muscles in the resting and not the contracted state, which is the case for hindlimb unloaded muscles. Further, emphasis has been placed on events within the capillary and across the RBC-subsarcolemmal boundary as elucidated by Federspiel and Popel, 1986 and Groebe and Thews, 1990, which is not considered in the original Krogh Cylinder Model. Despite elegant calculations that predict the limitation of O_2 transport in the plasma space (Ref. 35), recent studies with crocetin, a compound that enhances O_2 transport in plasma failed to improve O_2 conductance (Ref. 11). In a review article, Wagner, 2000 suggested that the reason for this is that there is adequate conductive mixing in the microcirculation. Richardson et al., 1995 provided experimental evidence that there is a steep O_2 gradient between the blood and myocyte and revealed that O_2 pressure in the blood is ~10 times higher than in the cytoplasm during exercise in humans. He supported the idea that the path between the red cell to the sarcolemma plays an important role in determining maximal muscle O_2 uptake (Ref. 36). Groebe and Thews (1990) suggested that extracellular and intracellular pO_2 diffusivities are different. They referred to the space containing plasma, capillary endothelium, and interstitial space as the "perierythrotic regions" and claimed that the diffusivity of this region has different diffusion properties than that within a myocyte (Ref. 37). For this reason, the chosen mathematical model was evaluated using a diffusivity value of the perierythrotic region ($D^T = 1.65\times10^{-5}$ cm^2/s), which has a high resistance as described by Groebe and Thews, 1990, and the diffusivity of the muscle fibers ($D^T = 3.04\times10^{-5}$ cm^2/s). However, the O_2 distribution in the model was found to be attributed mostly to the perfusion rate with the capillary density and diffusivity having less influence.

In the present model, we assumed that the O_2 uptake remains constant regardless of the fiber type transition that may occur in the muscle. This is contrary to that which actually occurs during spaceflight since slow twitch SOL muscles transition to fast-twitch muscles. After 5 weeks HU, the maximum rate of O_2 uptake in the SOL is decreased by 19 percent (Ref. 7). However, our purpose was to focus on the role of the circulatory system in a microgravity environment, though the inclusion of the changes in the fiber-type transition may be pursued in future work.

In the mathematical model described herein there was no region of the GAS that exhibited a pO_2^T<1.25 mmHg. However, the rat GAS muscle is reduced by 23 percent after 15 days of HU with 4 percent of this loss accounted for by the degeneration of the white GAS (Ref. 1). Hepple et al., 2000 showed a 45 percent reduction of GAS muscle fiber cross-sectional area when the absolute blood flow was reduced 30 percent in the canine model as a result of immobilization; however, the study did not investigate the changes in blood distribution within the muscle or the percentage of the type I fibers and whether they contributed to most of the degeneration (Ref. 38). The loss of GAS muscle could be caused by other factors in addition to O_2 depletion such as stress and diet. Portions of the red GAS may have become deoxygenated due to the disproportional distribution of blood flow. The depletion of O_2 may be part of the reason, but perhaps not the sole cause of the muscle degeneration.

The downregulation of protein synthesis observed in the hindlimb unloaded SOL muscle may be a consequence of an inadequate O_2 supply to the mitochondria which limits ATP production and, in turn, protein synthesis. In the rat SOL muscle the lack of O_2 inhibits protein synthesis and increases the rate of protein degradation (Ref. 39). In microgravity muscle degeneration can be attributed to protein loss primarily due to a decline in protein synthesis (Refs. 32 and 33). Given that the SOL muscle is composed of predominately slow-twitch fibers which rely on aerobic respiration and that the SOL muscle has less

blood when it is unloaded, it is possible that this is the reason that the SOL exhibits more degeneration than the GAS. This occurs in humans as well. In humans 6 months of weightlessness has been shown to lead to a loss of fiber mass, force, and power with the hierarchy of the effects being SOL type I > SOL type II > GAS type I > GAS type II (Ref. 40).

Conclusions

The model described herein predicts that the short-term simulated HU causes the rat SOL muscle to become hypoxic whereas the GAS maintains a normal tissue O_2 distribution. The depletion of O_2 may be, at least in part, an instigator of the degeneration of skeletal muscles. A reduced cabin partial pressure of O_2 may cause further muscle degeneration.

Appendix A.—Acronyms

C	oxygen concentration
C'	hemoglobin concentration
C_{sat}'	saturated concentration of oxygen bound to hemoglobin
D	diffusivity in the capillary
D^T	diffusivity in the tissue
H	Henrys Law constant in blood
H^T	Henrys Law constant in tissue
L	capillary length
m	slope of the oxygen-hemoglobin dissociation curve
M_T	mass of the tissue
n	oxygen flux
N	Hill Equation coefficient
nc	capillarity
pO_2	partial pressure of oxygen
$pO_2{}^T$	partial pressure of oxygen in the tissue
pO_{50}	partial pressure of oxygen at which 50 percent of the O_2 binding sites are filled
Q	volumetric flowrate of blood
r_a	radius at which the tissue becomes anoxic
r_C	capillary radius
r_T	tissue cylinder radius
r	radius in cylindrical coordinates
R	rate per unit volume of oxygen uptake
t	time
v_0	volume average velocity
V_T	volume of the tissue
Z	distance in z direction

Appendix B.—Derivation of Equations

After expanding Equation (3) the result is

$$\partial C/\partial t = D\left[\frac{1}{r}\frac{\partial}{\partial r}\left(r\frac{\partial C}{\partial r}\right)+\frac{1}{r^2}\frac{\partial^2 C}{\partial \theta^2}+\frac{\partial^2 C}{\partial z^2}\right]-v^0\left[\frac{1}{r}\frac{\partial}{\partial r}(rC)+\frac{1}{r}\frac{\partial C}{\partial \theta}+\frac{\partial C}{\partial z}\right]-R\,. \tag{B1}$$

We will refer back to Equation (B1). The Krogh model consists of (1) O_2 transport through blood and (2) reaction in tissues.

Tissue

Henry's law was used and Equation (B1) was simplified using the assumptions listed in the methods section so that

$$\frac{1}{r}\frac{d}{dr}\left(r\frac{dpO_2^T}{dr}\right)=\frac{RH^T}{D^T}\,. \tag{B2}$$

The properties of the tissue are denoted with a *T*. The boundary conditions were set for this equation. At the interface between the capillary and tissue the pO_2 is the same and the O_2 flux is continuous.

BC1: $r=r_c\,,\ pO_2=pO_2^T\,,\ D\dfrac{\partial pO_2}{\partial r}=D^T\dfrac{\partial pO_2^T}{\partial r}$

At the Krogh tissue cylinder diameter the flux is zero since there is a plane of symmetry between the cylinders.

BC2: $r=r_T\,,\ \partial pO_2^T/\partial r=0$

Equation (B2) was integrated twice and the boundary conditions BC1 and BC2 were applied.
Equation (4) is the result.

Capillary

Equation (B1) was simplified using the assumptions listed in the methods section so that

$$v_0\frac{\partial C}{\partial z}-D\left[\frac{1}{r}\frac{\partial}{\partial r}\left(r\frac{\partial C}{\partial r}\right)\right]=-R\,. \tag{B3}$$

Hemoglobin—Equation (B1) was simplified using the assumptions listed in the methods section where *C*' denotes the hemoglobin concentration so that

$$v_0\frac{\partial C'}{\partial z}=R_{HbO}\,. \tag{B4}$$

The slope of the oxygen hemoglobin curve is

$$m = \frac{\partial C'}{\partial C}. \tag{B5}$$

Combining Equations (B3) to (B5), recognizing $R = R_{HbO}$, and applying Henry's Law we have

$$\frac{\partial pO_2}{\partial z} = \frac{D}{v_0(1+m)}\left[\frac{1}{r}\frac{\partial}{\partial r}\left(r\frac{\partial pO_2}{\partial r}\right)\right]. \tag{B6}$$

The slope of the oxygen-hemoglobin curve can be expressed as a function of the Hill Equation coefficient, N, the partial pressure of O_2 at which 50 percent of the O_2 binding sites are filled, pO_{50}, Henry's Constant, H, the partial pressure of O_2 in the blood, pO_2, and the saturated concentration of O_2 bound to hemoglobin, C_{sat}' so that

$$m = NpO_2^{N-1}pO_{50}^{N}HC'_{sat}/\left[pO_{50}^{N} + pO_2^{N}\right]^2. \tag{B7}$$

A derivation of Equation (B7) may be found on page 242 in Fournier, R L. Basic transport phenomena in biomedical engineering. New York: Taylor & Francis, 2007 (Ref. 41).

The radial average of the capillary pO_2 was taken since the bulk of the oxygen mass transfer resistance is not within the capillary, but in the tissue. The radially averaged pO_2 level, $\langle pO_2 \rangle$, is the sum of many thin-walled annuluses with radii from 0 to r_c, each multiplied times their respective pO_2, divided by the entire area. Therefore, Equation (B6) becomes

$$\frac{1}{\pi r_c^2}\int_0^{r_c}\frac{\partial pO_2}{\partial z}\times 2\pi r\partial r = \frac{D}{v_0(1+m)}\frac{1}{\pi r_c^2}\int_0^{r_c}\frac{1}{r}\frac{\partial}{\partial r}\left(r\frac{\partial pO_2}{\partial r}\right)\times 2\pi r\partial r. \tag{B8}$$

The left-hand size of this equation resembles the radially averaged pO_2 level equation. The equation becomes

$$\frac{d}{dz}\langle pO_2\rangle = \frac{2D}{v_0(1+m)r_c}\frac{dpO_2}{dr}|_{rc}. \tag{B9}$$

After applying BC1 Equation (B9) becomes

$$\frac{d}{dz}\langle pO_2\rangle = \frac{2D^T}{v_0(1+m)r_c}\frac{dpO_2^T}{dr}|_{rc}. \tag{B10}$$

By differentiating Equation (4) $dpO_2^T/dr|_{rc}$ can be solved. Equation (B10) becomes

$$\frac{d}{dz}\langle pO_2\rangle = -\frac{RH^T}{v_0(1+m)}\left[\frac{r_T^2}{r_c^2}-1\right]. \tag{B11}$$

Equation (B11) was integrated to find the axial change in the capillary oxygen partial pressure, Equation (7).

References

1. McDonald, K.S., Delp, M.D. and Fitts, R.H. (1992) Fatigability and Blood Flow in the Rat Gastrocnemius-Plantaris-Soleus after Hindlimb Suspension. *J Appl Physiol* 73: 1135-40.
2. McDonald, K.S., Delp, M.D. and Fitts, R.H. (1992) Effect of Hindlimb Unweighting on Tissue Blood Flow in the Rat. *J Appl Physiol* 72: 2210-8.
3. Morey-Holton, E.R. and Globus, R.K. (1998) Hindlimb Unloading of Growing Rats: A Model for Predicting Skeletal Changes During Space Flight. *Bone* 22: 83S-88S.
4. Pavy-Le Traon, A., Heer, M., Narici, M.V., Rittweger, J. and Vernikos, J. (2007) From Space to Earth: Advances in Human Physiology from 20 Years of Bed Rest Studies (1986-2006). *Eur J Appl Physiol* 101: 143-94.
5. Bloomfield, S.A. (2006) Does Altered Blood Flow to Bone in Microgravity Impact on Mechanotransduction? *J Musculoskelet Neuronal Interact* 6: 324-6.
6. Colleran, P.N., Wilkerson, M.K., Bloomfield, S.A., Suva, L.J., Turner, R.T. and Delp, M.D. (2000) Alterations in Skeletal Perfusion with Simulated Microgravity: A Possible Mechanism for Bone Remodeling. *J Appl Physiol* 89: 1046-54.
7. Desplanches, D., Mayet, M.H., Sempore, B. and Flandrois, R. (1987) Structural and Functional Responses to Prolonged Hindlimb Suspension in Rat Muscle. *J Appl Physiol* 63: 558-63.
8. Whalen, W.J., Buerk, D. and Thuning, C.A. (1973) Blood Flow-Limited Oxygen Consumption in Resting Cat Skeletal Muscle. *Am J Physiol* 224: 763-8.
9. Holloszy, J.O. (1967) Biochemical Adaptations in Muscle. Effects of Exercise on Mitochondrial Oxygen Uptake and Respiratory Enzyme Activity in Skeletal Muscle. *J Biol Chem* 242: 2278-82.
10. Behnke, B.J., McDonough, P., Padilla, D.J., Musch, T.I. and Poole, D.C. (2003) Oxygen Exchange Profile in Rat Muscles of Contrasting Fibre Types. *J Physiol* 549: 597-605.
11. Wagner, P.D. (2000) Diffusive Resistance to O2 Transport in Muscle. *Acta Physiol Scand* 168: 609-14.
12. Papadopoulos, S., Endeward, V., Revesz-Walker, B., Jurgens, K.D. and Gros, G. (2001) Radial and Longitudinal Diffusion of Myoglobin in Single Living Heart and Skeletal Muscle Cells. *Proc Natl Acad Sci U S A* 98: 5904-9.
13. Roudier, E., Gineste, C., Wazna, A., Dehghan, K., Desplanches, D. and Birot, O. (2010) Angio-Adaptation in Unloaded Skeletal Muscle: New Insights into an Early and Muscle Type-Specific Dynamic Process. *J Physiol* 588: 4579-91.
14. Gray, S.D. (1988) Histochemical Analysis of Capillary and Fiber-Type Distributions in Skeletal Muscles of Spontaneously Hypertensive Rats. *Microvasc Res* 36: 228-38.
15. Vaupel, P. (1976) Effect of Percentual Water Content in Tissues and Liquids on the Diffusion Coefficients of O2, Co2, N2, and H2. *Pflugers Arch* 361: 201-4.
16. Homer, L.D., Shelton, J.B., Dorsey, C.H. and Williams, T.J. (1984) Anisotropic Diffusion of Oxygen in Slices of Rat Muscle. *Am J Physiol* 246: R107-13.
17. Edwards, M.J., Novy, M.J., Walters, C.L. and Metcalfe, J. (1968) Improved Oxygen Release: An Adaptation of Mature Red Cells to Hypoxia. *J Clin Invest* 47: 1851-7.
18. Ding, Z. and Fournier, R.L. (2002) Oxygen and Inulin Transport Measurements in a Planar Tissue-Engineered Bioartificial Organ. *Tissue Eng* 8: 25-36.
19. Fisher, A.J., Schrader, N.W. and Klitzman, B. (1992) Effects of Chronic Hypoxia on Capillary Flow and Hematocrit in Rat Skeletal Muscle. *Am J Physiol* 262: H1877-83.
20. McGuire, B.J. and Secomb, T.W. (2001) A Theoretical Model for Oxygen Transport in Skeletal Muscle under Conditions of High Oxygen Demand. *J Appl Physiol* 91: 2255-65.
21. Wagatsuma, A. (2008) Effect of Hindlimb Unweighting on Expression of Hypoxia-Inducible Factor-1alpha Vascular Endothelial Growth Factor, Angiopoietin, and Their Receptors in Mouse Skeletal Muscle. *Physiol Res* 57: 613-20.
22. Duling, B.R. and Berne, R.M. (1970) Longitudinal Gradients in Periarteriolar Oxygen Tension. A Possible Mechanism for the Participation of Oxygen in Local Regulation of Blood Flow. *Circ Res* 27: 669-78.

23. Richmond, K.N., Burnite, S. and Lynch, R.M. (1997) Oxygen Sensitivity of Mitochondrial Metabolic State in Isolated Skeletal and Cardiac Myocytes. *Am J Physiol* 273: C1613-22.
24. Degens, H., Deveci, D., Botto-van Bemden, A., Hoofd, L.J. and Egginton, S. (2006) Maintenance of Heterogeneity of Capillary Spacing Is Essential for Adequate Oxygenation in the Soleus Muscle of the Growing Rat. *Microcirculation* 13: 467-76.
25. Gerard, D.F., Gausewitz, S.H., Dilley, R.B. and Bernstein, E.F. (1981) Acute Physiologic Effects of Arteriovenous Anastomosis and Fistula in Revascularizing the Ischemic Canine Hind Limb. *Surgery* 89: 485-93.
26. Nicogossian, A.E. (1993) *Space Biology and Medicine*, (American Institute of Aeronautics and Astronautics & Nauka Press: Washington, D.C. & Moscow).
27. Diedrich, A., Paranjape, S.Y. and Robertson, D. (2007) Plasma and Blood Volume in Space. *Am J Med Sci* 334: 80-5.
28. Kandarian, S.C., Boushel, R.C. and Schulte, L.M. (1991) Elevated Interstitial Fluid Volume in Rat Soleus Muscles by Hindlimb Unweighting. *J Appl Physiol* 71: 910-4.
29. Ustunel, I. and Demir, R. (1997) A Histochemical, Morphometric and Ultrastructural Study of Gastrocnemius and Soleus Muscle Fiber Type Composition in Male and Female Rats. *Acta Anat (Basel)* 158: 279-86.
30. Hudlicka, O. (1975) Uptake of Substrates in Slow and Fast Muscles in Situ. *Microvasc Res* 10: 17-28.
31. Boutilier, R.G. and St-Pierre, J. (2000) Surviving Hypoxia without Really Dying. *Comp Biochem Physiol A Mol Integr Physiol* 126: 481-90.
32. Fitts, R.H., Riley, D.R. and Widrick, J.J. (2000) Physiology of a Microgravity Environment Invited Review: Microgravity and Skeletal Muscle. *J Appl Physiol* 89: 823-39.
33. Thomason, D.B., Biggs, R.B. and Booth, F.W. (1989) Protein Metabolism and Beta-Myosin Heavy-Chain Mrna in Unweighted Soleus Muscle. *Am J Physiol* 257: R300-5.
34. Ellis, C.G., Potter, R.F. and Groom, A.C. (1983) The Krogh Cylinder Geometry Is Not Appropriate for Modelling O2 Transport in Contracted Skeletal Muscle. *Adv Exp Med Biol* 159: 253-68.
35. Federspiel, W.J. and Popel, A.S. (1986) A Theoretical Analysis of the Effect of the Particulate Nature of Blood on Oxygen Release in Capillaries. *Microvasc Res* 32: 164-89.
36. Richardson, R.S., Noyszewski, E.A., Kendrick, K.F., Leigh, J.S. and Wagner, P.D. (1995) Myoglobin O2 Desaturation During Exercise. Evidence of Limited O2 Transport. *J Clin Invest* 96: 1916-26.
37. Groebe, K. and Thews, G. (1990) Calculated Intra- and Extracellular Po2 Gradients in Heavily Working Red Muscle. *Am J Physiol* 259: H84-92.
38. Hepple, R.T., Hogan, M.C., Stary, C., Bebout, D.E., Mathieu-Costello, O. and Wagner, P.D. (2000) Structural Basis of Muscle O(2) Diffusing Capacity: Evidence from Muscle Function in Situ. *J Appl Physiol* 88: 560-6.
39. Fagan, J.M. and Tischler, M.E. (1989) Effects of Oxygen Deprivation on Incubated Rat Soleus Muscle. *Life Sci* 44: 677-81.
40. Fitts, R.H., Trappe, S.W., Costill, D.L., Gallagher, P.M., Creer, A.C., Colloton, P.A., Peters, J.R., Romatowski, J.G., Bain, J.L. and Riley, D.A. (2010) Prolonged Space Flight-Induced Alterations in the Structure and Function of Human Skeletal Muscle Fibres. *J Physiol* 588: 3567-92.
41. Fournier, R.L. (2007) *Basic Transport Phenomena in Biomedical Engineering*, (Taylor & Francis New York).